

***In vivo* Model of Crystal-Associated Osteoarthritis**

¹Ahmed M. Elmesiry, ²Magdi A. Seleim and ³David Cullis-Hill

¹Diagnostic Imaging and Endoscopy Unit, Animal Reproduction Research Institute,
Agriculture Research Center, 12556 Haram, Giza, Egypt

²Department of Surgery, Faculty of Veterinary Medicine,
Kafrelsheikh University, 33156 Kafrelsheikh, Egypt

³Sylvan Scientific Pty Ltd, 111 Bronte Rd, Bondi Junction, Sydney, NSW 2022, Australia

Abstract: Crystals are common components of synovial fluids from degenerated joints and often accompany unusually severe cartilage destruction. To date, no ideal osteoarthritis (OA) animal model with crystal formation has been described. In The present study, a new osteoarthritis model was developed accompanied by crystal formation. The radio carpal joints of the right forelimb of 12 donkeys were injected with 100mg Allogeneous cartilage powder (group A) or vehicle treatment (Group B) for 8 injections over a period of 70 days. (n=six per group). Osteoarthritis was evaluated by weekly examination of Lameness score, carpal circumference, joint flexion angle, Synovial fluid analysis (total protein, calcium, phosphorus, magnesium and WBC count) in addition to light and scanning electron microscopy for cartilage and synovial membrane at day 70. Lameness score and joint circumference was increased in-groups A however joint flexion angle was decreased compared to group B ($P<0.05$). Synovial fluid calcium, phosphorus, magnesium, total protein and leukocyte count were increased in group A compared to group B. Cartilage damage was observed grossly, histologically in Groups A together with synovial membrane fibrosis. SEM revealed formation of joint crystals adhering to the synovial membrane in-group A injected joints. Allogeneous cartilage powder injection in the donkey is a suitable model to be investigated as a viable alternative OA associated crystals model.

Key words: Joint Crystals • Osteoarthritis • Cartilage • Equine

INTRODUCTION

Osteoarthritis (OA) is a common disease of joints and among the most important causes of pain, disability and economic loss in all populations affecting over 10% of the people [1]. Osteoarthritis (OA) is the most common disease affecting the joints in humans and among the most important causes of pain, disability and economic loss in all populations [2, 3].

The disease status in the United states was 21 million in 1995, which rise to 27 million in Lawrence *et al.* [4]. however in the European Union the affected people reached 100 million in Altman *et al.* [5].

OA may be considered as a group of disorders characterized by progressive deterioration of the articular cartilage accompanied by changes in the bone and soft tissues of the joint. Synovitis and joint effusion are often

associated with the disease and, clinically, the disease is characterized by pain and dysfunction of the affected joint [3].

Animal models are a research tool used to study the pathogenesis, diagnosis and new therapeutic drugs of many different diseases. The different types of arthritis models have been previously reviewed [6-8].

Recently, The advantage of the horse as a model of naturally occurring osteoarthritis has been described [9]. Equine OA share many features with human OA as the disease causes, pathogenesis, diagnosis and therapeutic treatments.

The use of cartilage particles to induce osteoarthritis was previously described in dog [10], rabbit [11] and donkey [12]. A combination of intra-articular injection of cartilage particles, arthroscopic partial thickness cartilage defect and exercise have been used to create a

model of degenerative joint disease in the horse [13]. The fate and effects of surgically implanted osteochondral fragments on the middle carpal joint of horses subjected to exercise were investigated [14].

Calcium-containing crystals that encompass calcium pyrophosphatedihydrate (CPPD) and basic calcium phosphate (BCP) crystals are associated with several diseases in human and animals such as acute joint inflammation and destructive arthropathies. They are detected in 100% of OA synovial fluid, of OA meniscus and in all knee and hip OA cartilage harvested at the time of arthroplasty. BCP crystals, including carbonated-substituted hydroxyapatite, tricalcium phosphate, octacalcium phosphate and magnesium whitlockite are heterogeneous in terms of structure, chemical composition and biological properties [15].

Studying of crystal-associated arthropathy was always depend on synovial fluid and cartilage sampling from human clinical cases [16] or injecting an in-vitro prepared crystals to healthy joints in laboratory animals [17].

This study is the continuation of our previous work [12] on development of a model of degenerative joint disease in the donkey that demonstrate clinical and morphological evidence of the onset, progression and crystal formation of OA. We hypothesized that injections of large doses allogeneous cartilage particles and exercise would result in clinical, histopathologic changes characteristic for osteoarthritis.

MATERIALS AND METHODS

Animals: The present study was performed with 13 healthy male donkeys (*Equus asinus*) weighting from 150 to 200 kg. Animals were housed in indoor stalls and fed on a maintenance ration of mixed grain with hay and unlimited water. All donkeys were dewormed with ivermectin 200 mcg/kg⁻¹ body weight.

Prior to inclusion in the study, lameness examination, body condition, radiographs of carpal joints, range of motion of carpal joints (angle of flexion) and evidence of joint effusion were assessed to ensure that all previous variables were within normal limits (baseline measurement).

Allogeneous Cartilage Particles (ACP): One local breed donkey weight 150 kg was euthanized. Pure articular cartilage was removed from the shoulder, carpal, fetlock, pastern, hock and stifle joints in a biosafety cabinet under aseptic conditions. The pooled cartilage was powdered

under liquid nitrogen in a mortar, producing particles as small as 20 mm in diameter (able to pass easy through a 14-gauge needle). These particles were resuspended at a concentration of 50mg/ml in a physiological saline solution contained amikacinsulfate[®] (50mg/ml). An aliquot of the suspension was cultured for 72hour on ordinary media to confirm sterility. The cartilage stock solution was stored on a fridge (4°C) until use.

Study Design: The 12 remaining donkeys were randomly divided in to 2 equal group (n= 6). Animals sedated with Xylazine Hcl[™] in a dose of 1 mg/kg. The skin was aseptically prepared for arthrocentesis of each right radiocarpal joint to obtain synovial sample for baseline analysis. Group A received 100mg(2 mLACP) (ACP group), Group B received the suspended solution (2mL) without add cartilage (Vehicle - Control group) intra-articular into the right radiocarpal joint using a 14G needle. These injections were repeated at 7, 14, 21, 28, 35, 42 and 56 days. The left radiocarpal joint remain intact to allow accurate lameness evaluation for the right for elimb. Donkeys were trotted for 15 min/day on soft ground 5 days each week until the end of the study. All Groups were euthanized at day 70 (Figure 1).

Outcome Measures

Clinical Examination: Clinical examinations of right forelimbs were performed weekly from day 0 (baseline) throughout the study period. Donkeys evaluated for lameness score on a scale 0 to 5 according to American Association of Equine Practitioners (AAEP) grading system (0: Lameness not perceptible under any circumstances, 1:Lameness is difficult to observe and is not consistently apparent, regardless of circumstances, 2: Lameness is consistently apparent under certain circumstances, 3: Lameness is consistently observable at a trot under all circumstances, 4: Lameness is obvious at a walk. 5:Lameness produces minimal weight bearing in motion) [18]. Circumference of the carpal joint was obtained at the proximal aspect of the carpus by using of a measurement tape (in cm). The tape measure placed over the proximal row of the carpal bones (accessory, radial, ulnar and intermediate carpal bones) with limb fully weight-bearing [19]. Maximum carpal flexion was measured by slowly flexing the carpus until the donkey resisted. The angle was then measured in degrees with goniometer [19]. A professor of large animal surgery (Lameness specialist) assessed all clinical outcome variables without known of the treatment assignment.

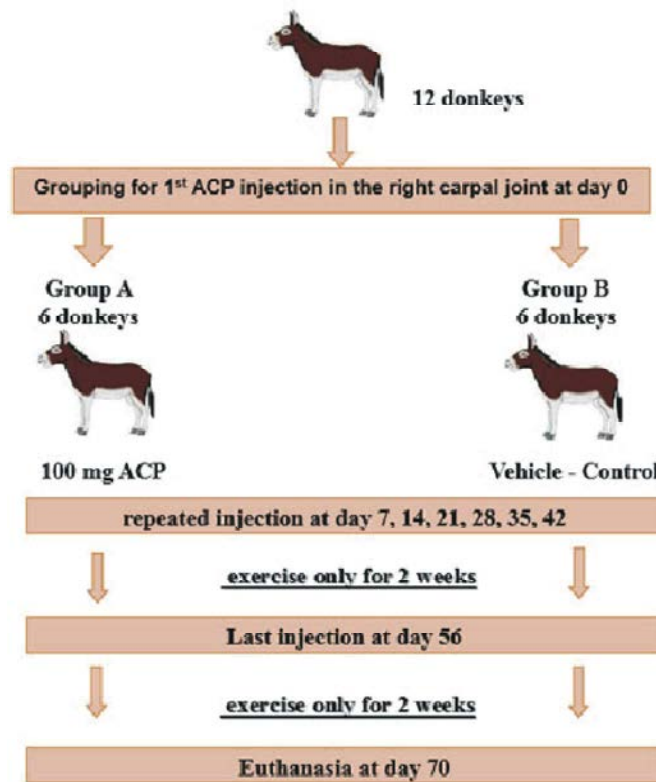


Fig. 1: Flowchart of the study protocol explaining the grouping, injection time and euthanasia.

Synovial Fluid Analysis: Synovial fluid sample (1 to 2mL) aseptically aspirated from each right radio carpal joint at day 0 (baseline analysis) and before each injection. The conventional analysis of synovial fluid included assessment of total protein concentration, white blood cell (WBC) count, Calcium, Phosphorus and Magnesium. Total protein concentrations and WBC were determined via Double Beam UV Visible Spectrophotometer and use of an automated cell counter, respectively [20]. A clinical pathologist who was blinded to the treatment protocol did all the synovial analyses.

Gross Pathology of Joint Tissue: Animals were euthanized by administration of pentobarbitone sodium^{iv} (100 mg/kg IV) and tissue samples collected from joint capsule and articular cartilage (Figure 2). Carpal joints specifically examined for degree and location of articular cartilage fibrillation or erosion. A subjective grade (scale of 0 to 4) assigned for partial- and full-thickness cartilage erosion as well as synovial membrane hemorrhage. A total erosion score assigned, also with a scale of 0 to 4. For each of the 2 variables, grade 0 represented no pathological change and 4 represented a severe change. Each joint also assessed for the presence of synovial adhesions [21].

Light Microscopy: Specimens from the synovial membrane and joint capsule were harvested from the area located close to the joint space and placed in neutral-buffered 10% formalin (NBF) stained with H&E and examined microscopically. Samples evaluated for cellular infiltration, synovial intimal hyperplasia, subintimal edema, subintimal fibrosis and subintimal vascularity. Each variable was graded and reported as a numeric value 0 to 4 (0 = normal, 1 = slight change, 2 = mild change, 3 = moderate change and 4 = severe change [21].

Full thickness articular cartilage samples of 5-mm² diameter were obtained from each joint (Figure 2). Sampling sites were chosen to represent an area of dorsal cartilage (C1&C3) and palmar cartilage (C2& C4) regions. Samples placed in (NBF) for 7 days and then placed in 10% EDTA for 21 days for decalcification then processed routinely to paraffin wax for histological examination by a professor of pathology who was unaware of treatment assignment. Samples were sliced into 5-µm sections and stained with H&E, cartilage were graded on a scale of 0 to 6 (Grade 0: Smooth, Grade 1: Surface irregular, Grade 2: Surface discontinuous, Grade 3: Vertical fissure, Grade 4: Erosion, Grade 5: Denudation, Grade 6: Deformation) [22].

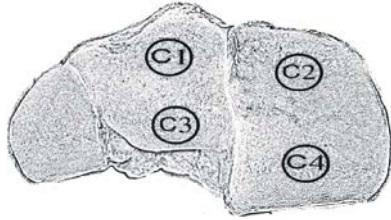


Fig. 2: Illustration of cartilage collection sites from distal articular surface of the radius. C1&C3 represented samples for the Light microscopy while C2&C4 for the SEM

Scanning Electron Microscopy: Cartilage C2&C4 pieces which obtained from the distal radial surface of each right carpal joint as well as synovial membrane. Specimens were fixed in 2.5% (v/v) glutaraldehyde solution in phosphate buffer saline (PBS pH 7.4) for approximately 24 h, followed by thorough washing using multiple changes of PBS. Secondary fixation in a solution of 1% (w/v) osmium tetroxide in PBS for 1.5 h. Specimens were again rinsed in multiple changes of PBS then dehydrated with an ascending ethanol series 50%, 60%, 70%, 80%, 90%, 100%, followed by pure, dry acetone. This followed immediately by critical point drying with liquid carbon dioxide then coated with gold and examined by a professor of pathology using scanning electron microscope^v. Cartilage surface was examined for erosion and micro cracks on a scale of 0 to 4 (grade 0= normal; grade 1= malacia; grade 2; superficial cracks; grade 3= fibrillation; grade 4= full thickness erosion) [23]. Synovial membranes were graded on a scale of 0 to 4 according to the percentage of affected area (Grade 0 = normal; grade 1= 0-25% affected; grade 2= 25-50; grade 3= 50-75; grade 4= 75-100).

Statistical Analysis: Data was assessed for normality using the Shapiro-Wilk test for normality and outliers. Normality was examined graphically for skewness or kurtosis within group variances to look at the homogeneity of variance. The two groups were compared on weekly after initiation of injection. Variables including carpal flexion angle, carpal circumference, TP and TWBC were analyzed using independent samples T- test. Lameness score, gross pathological and histo-pathologic scores were analyzed using independent samples Mann-Whitney U Test. $P < 0.05$ was considered significant. Values are reported as mean \pm standard deviation. All statistical analysis were done using IBM SPSS software Version 23^{vi}.

RESULTS

Clinical Examination

Lameness Score: Increasing in the lameness score begin at day 14 for ACP group (mean \pm SD, 1.67 ± 0.52) and peak at day 21 (3 ± 0). At day 70, the lameness score was at lowest value, 1.33 ± 0.52 for ACP Group. Vehicle control group had no lameness all over the study period (Figure 3-A). There was a significant difference between ACP group and vehicle control group ($P < 0.05$) from day 14 to the end of the study. Carpal circumference was increased in both groups reached its peak at day 35 for ACP group (24.33 ± 1.29), vehicle control group (23.1 ± 0.45). From day 56, the circumference was constant to the study end (day 70), 23.67 ± 1.03 for ACP group and vehicle control group 23.1 ± 0.45 . There was a significant difference between ACP group and vehicle control group ($P < 0.05$) from day 14 to the end of the study (Figure 3-B). The flexion angle begin to decrease at day 7 in ACP group reaching its peak at day 35 (126.67 ± 5.16). At day 70, the flexion angle was at highest value, 146.67 ± 5.16 for ACP group. Vehicle control group had a constant 156.67 ± 2.58 throughout the study period (Figure 3-C). At day 21, 28, 35, 42 and 56 ACP group was significantly different from vehicle control group ($P < 0.05$). However, at day 70, there was no significant differences between both groups.

Synovial Fluid Analysis: Synovial WBCs count was increased in ACP group (333 ± 51.64 cells/ μ L) and vehicle control group (266.67 ± 51.64 cells/ μ L), after the first injection throughout the study. There was a significant difference between ACP group and vehicle control group ($P < 0.05$) from day 7 to the end of the study. Total protein also increased in ACP group (3.43 ± 0.58 g/dL) and vehicle control group (2.1 ± 0.15 g/dL) after the first injection throughout the study. There was a significant difference between ACP group and vehicle control group ($P < 0.05$) from day 7 to the end of the study. Magnesium increased in ACP group (2.1 ± 0.3 g/dL) and vehicle control group (1.5 ± 0.2 g/dL) after the first injection reaching its peak at day 70 (4.3 ± 0.3 for ACP group and 1.5 ± 0.2 for vehicle control group). There was a significant difference between ACP group and vehicle control group ($P < 0.05$) from day 7 to the end of the study (figure 4A). Phosphorus increased in ACP group (10.4 ± 1 g/dL) and vehicle control group (8.7 ± 1.4 g/dL) after the first injection reaching its peak at day 70 (13.3 ± 0.8 for ACP group and 8.7 ± 1.4 for vehicle control group). There was a significant difference between ACP group and vehicle control group ($P < 0.05$).

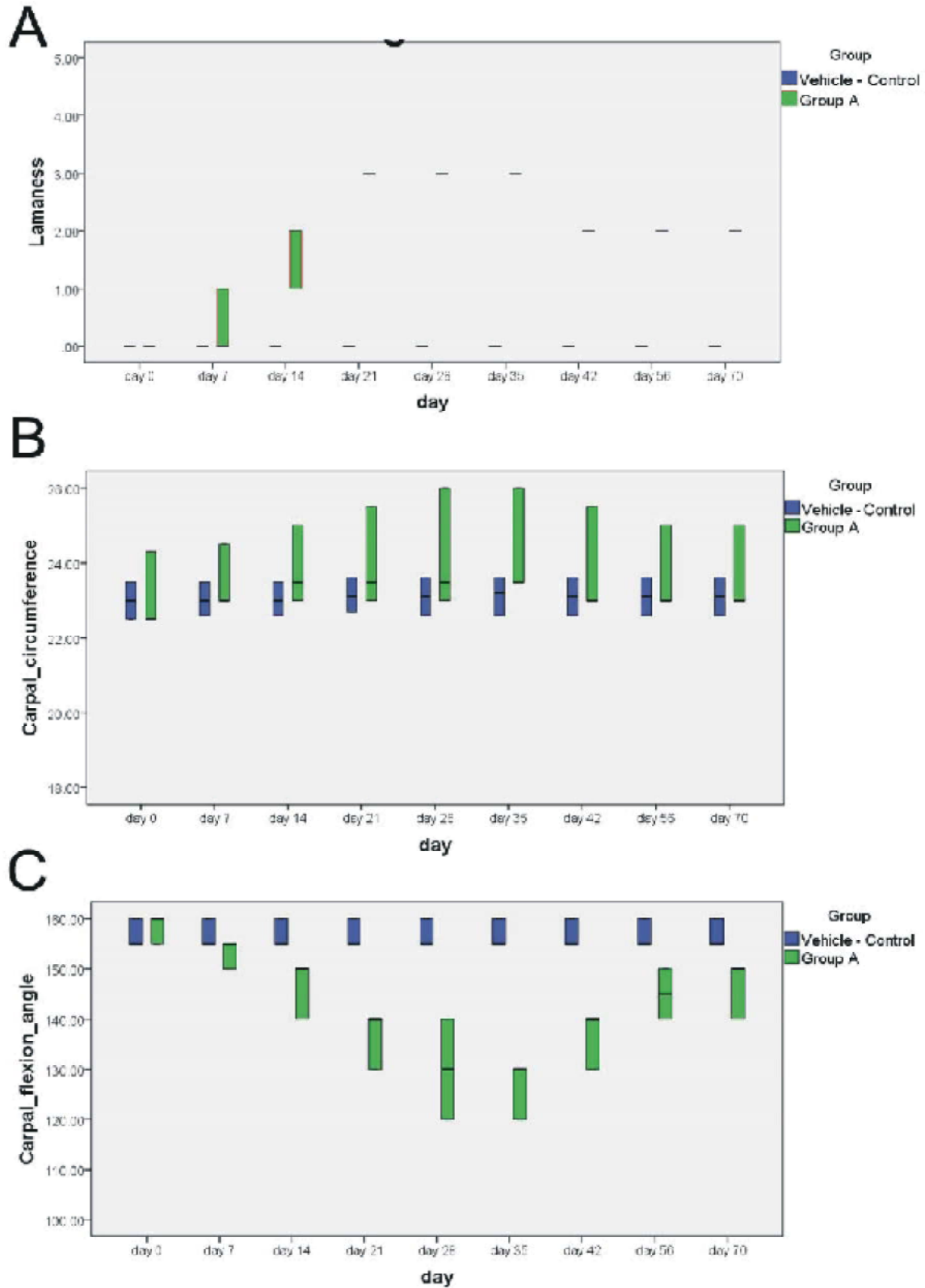


Fig. 3: Representative box plots of the lameness score, carpal circumference and joint flexion angle for group A and B over the study time period

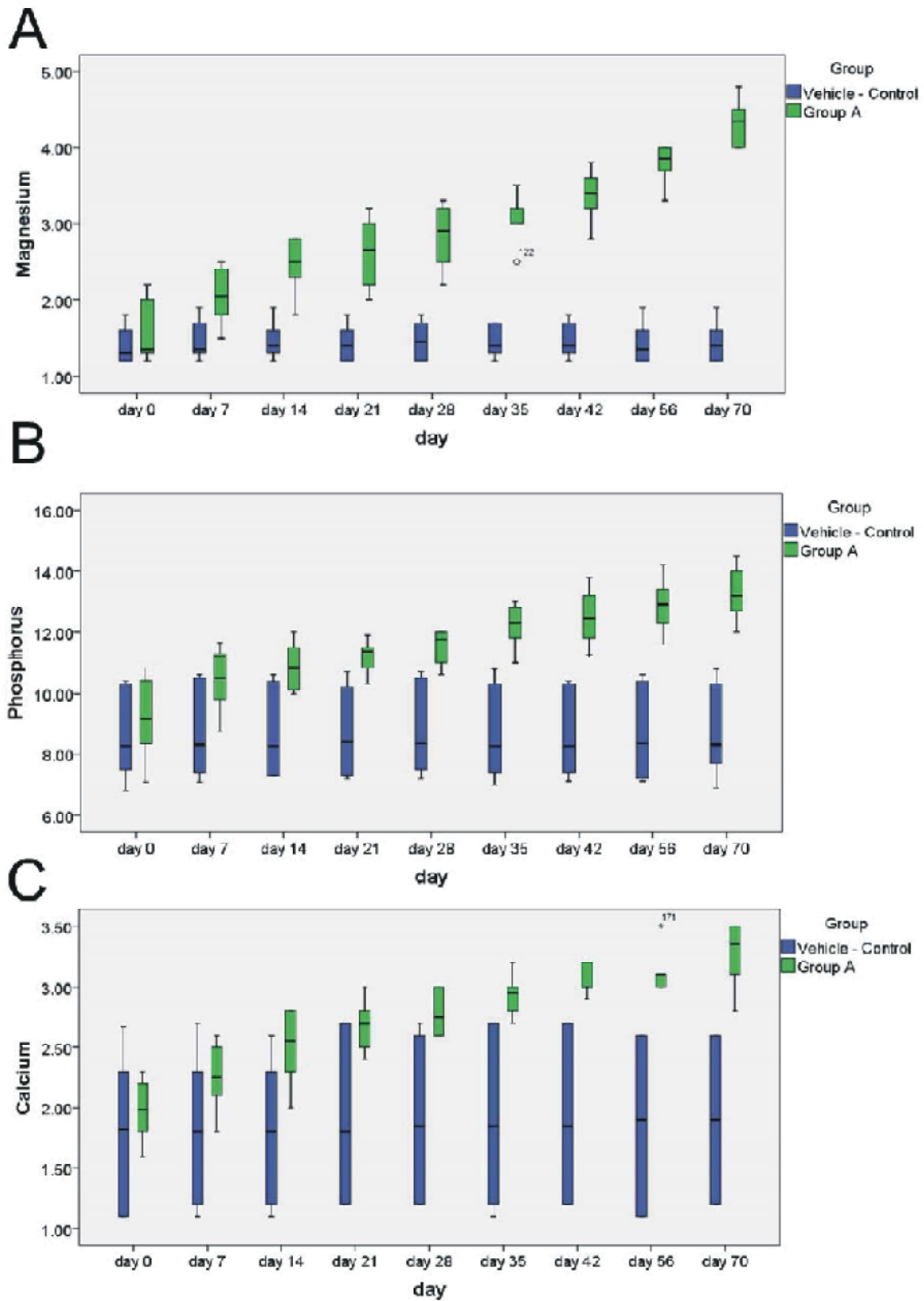


Fig. 4: Representative box plots of the calcium, magnesium and phosphorus for group A and B over the study time period

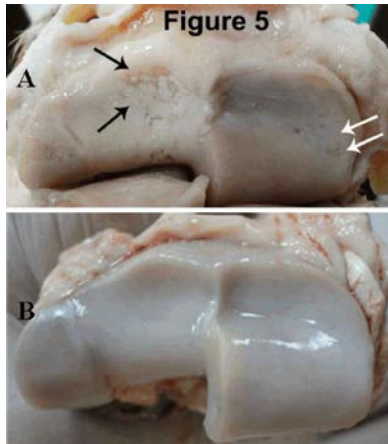


Fig. 5: Representative images of the gross morphology of the distal articular surface of the radius of Group A and B. black arrows refer to full thickness erosion however the white arrows refer to partial thickness erosion

from day 7 to the end of the study (Figure 4B). Calcium increased in ACP group (2.3 ± 0.3 g/dL) and vehicle control group (1.8 ± 0.6 g/dL) after the first injection reaching its peak at day 70 (3.3 ± 0.2 for ACP group and 1.9 ± 0.6 for vehicle control group). There was a significant difference between ACP group and vehicle control group ($P < 0.05$) from day 7 to the end of the study (Figure 4C).

Gross Pathology: ACP group had partial and full thickness erosion (2.67 ± 0.52) with a significant difference from vehicle control group ($P = 0.002$) (Figure 5). The synovial membrane had significantly difference between both groups ($P = 0.002$). ACP group had a synovial membrane adhesion.

Light Microscopy of Synovial Membrane: Induction of osteoarthritis did not result in significant change in synovial membrane intimal hyperplasia or subintimal edema (ACP group had slight changes 1 ± 0). Synovial membrane cellular infiltration was increased in ACP group (3.33 ± 0.52). ACP group was significantly different from vehicle control group ($P = 0.002$), ACP group characterized by large cartilage particles embedded inside the subintimal layer surrounded by a severe zone of cellular infiltration (Figure 6-A). Synovial membrane vascularity was increased in ACP group (2.67 ± 0.52). ACP group were significantly different from vehicle control group ($P = 0.002$). Synovial membrane fibrosis was increased in ACP group (2.67 ± 0.52). ACP group was significantly different from vehicle control group ($P = 0.002$).

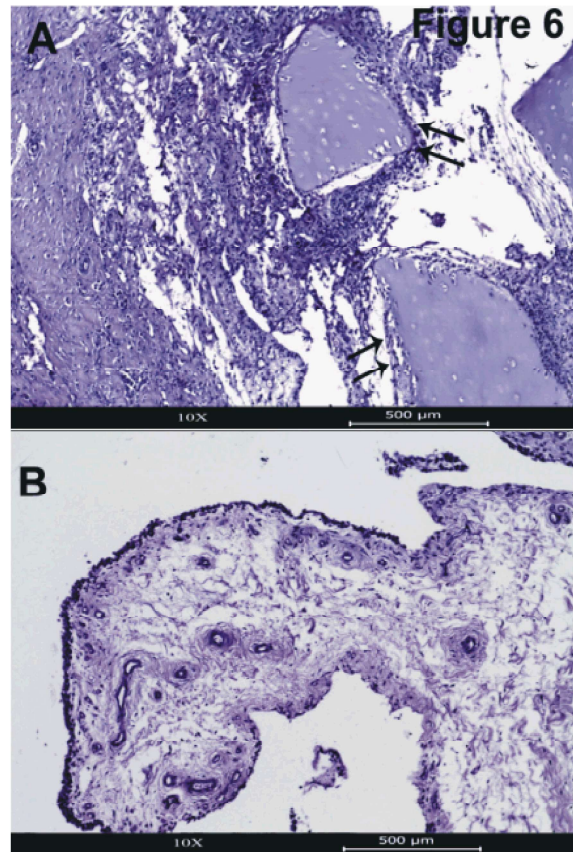


Fig. 6: Representative images of the light microscopy of the synovial membrane of Group A and B. black arrows refer to embedded cartilage particles inside the subintimal layer surrounded by a severe zone of cellular infiltration however white arrows refer to the subintimal blood vessels.

Light Microscopy of Articular Cartilage: Histologic evaluation of sample C1 via H&E revealed a significant increase in OA score for ACP group from vehicle control group ($P = 0.002$). C1 histologic score revealed more damage than C3 although this difference was not significant ($P = 0.518$). Lesion on ACP group (C1&C3: 5.67 ± 0.52), includes denudation (microfracture limited to bone surface) and deformation (bone remodeling includes: microfracture with fibrocartilaginous and osseous repair extending above the previous surface) (Figure 7-A). Vehicle control group revealed normal architecture and appropriate orientation of the Cells (Figure 7-B).

Scanning Electron Microscopy of Synovial Membrane: Induction of osteoarthritis revealed severe changes to the synovial membrane of ACP group (4 ± 0) which appeared

fibrotic compared to vehicle control group, which appeared normal. However ACP group was distinguished by formation of crystals adhering to the synovial membrane (Figure 8-A). There were significant differences in synovial intimal fibrosis between both groups ($P = 0.001$).

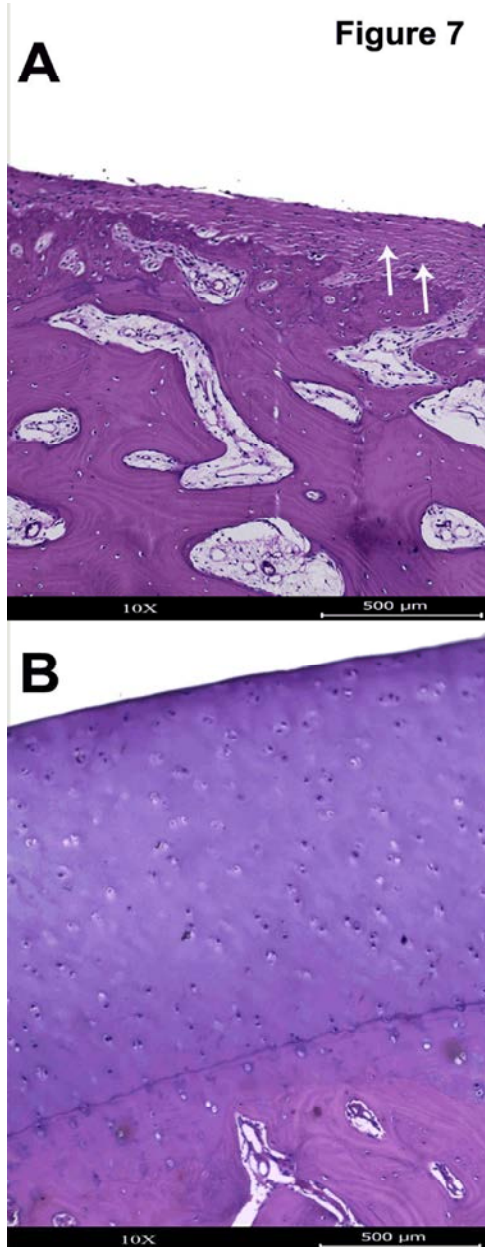


Fig. 7: Representative images of the light microscopy of the articular cartilage of groups A and B. white arrows refer to fibrocartilaginous and osseous repair extending above the subchondral bone however black arrows refer to matrix vertical fissures and erosions extending into the mid zone

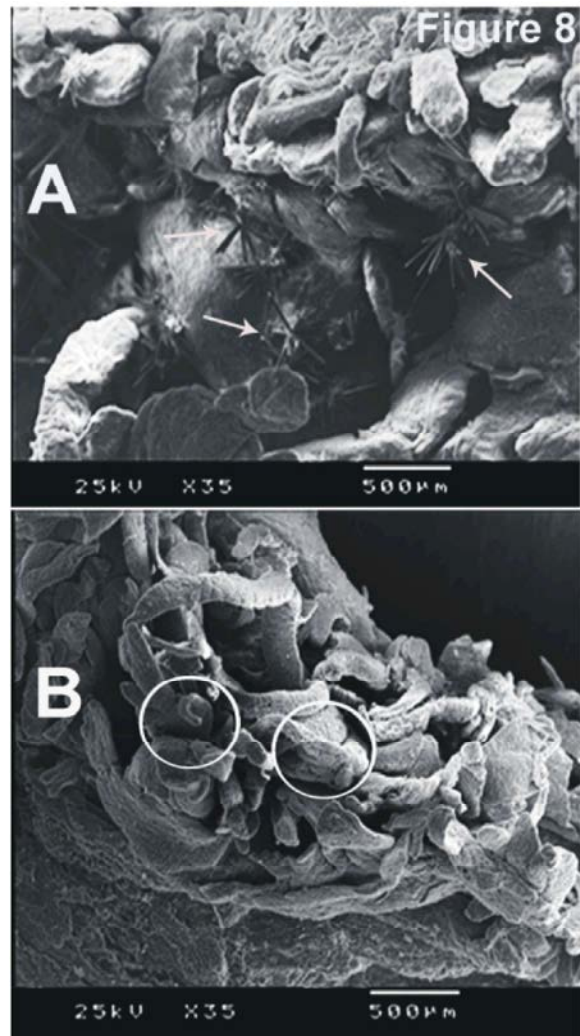


Fig. 8: Representative images of the SEM of synovial membrane of Groups A and B. white arrows refer to the synovial crystals, white circles refer to normal synovial villi and black circles refer to fibrotic zones

Scanning Electron Microscopy of Cartilage Surface:

ACP group had marked changes on the cartilage surface ($P=0.001$) compared with vehicle control group which appeared to be normal. Examination of cartilage surface at low magnification (35X) revealed normal architecture (vehicle control group). ACP group had full thickness cartilage fissures passed through the articular surface and penetrated deeply into the radial zone and sometimes to the level of the subchondralbone (4 ± 0). Vehicle control group was constantly normal. C2 & C4 histologic score revealed the same damaged with respect to their anatomical sites (Figure 9).

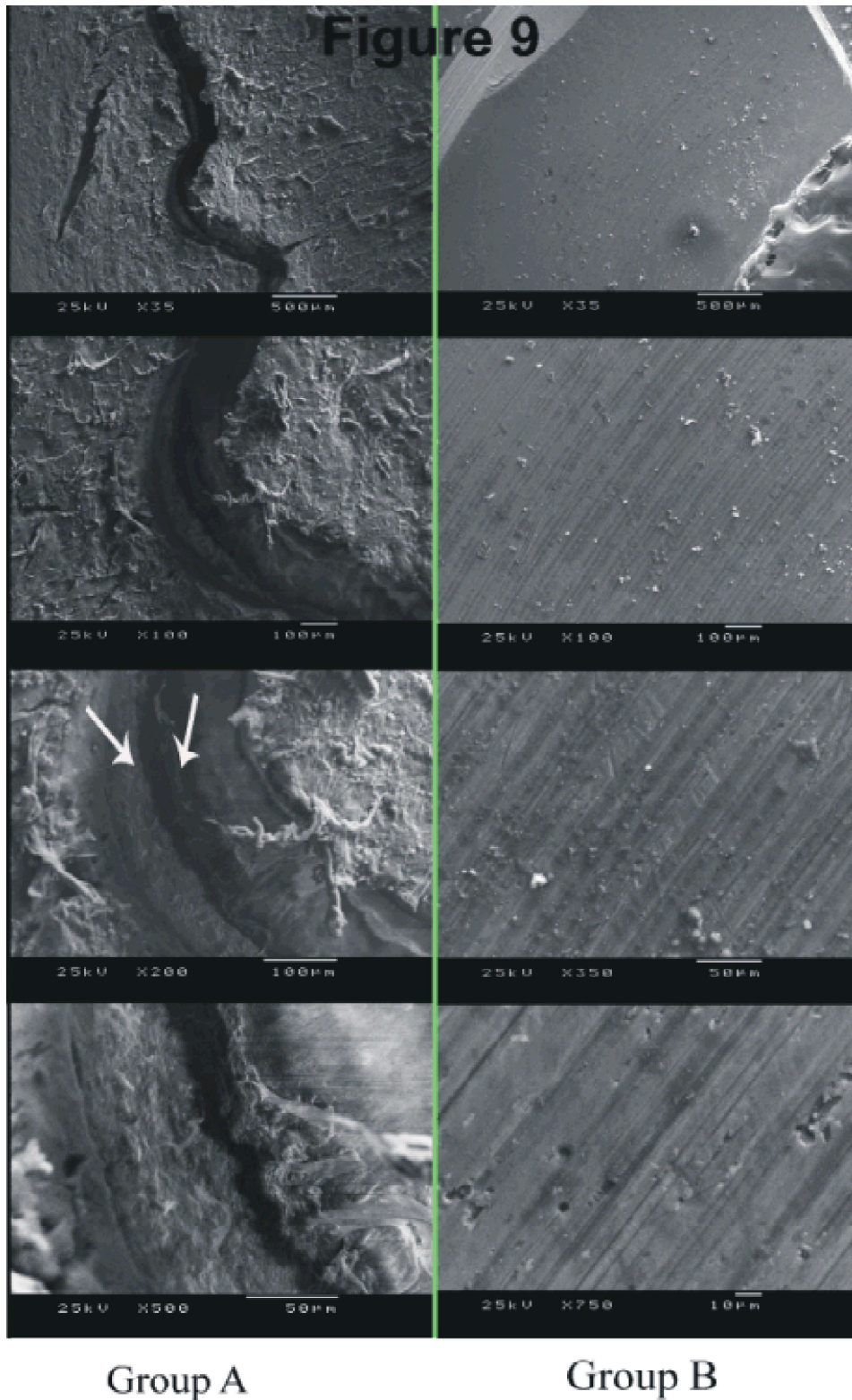


Fig. 9: Representative Series of magnified images of the articular cartilage SEM for Groups A and B. white arrows refer to deep cartilage fissure extending to the level of the subchondral bone however; black arrows refer to separation of the tangential lamellae

DISCUSSION

Crystals formation in joints is frequently associated with osteoarthritis (OA). Although the presence of intraarticular crystals has been correlated with severe joint pathology, it is still controversial whether such crystals are a primary cause of arthritis or a secondary consequence of joint damage [24, 25] and the mechanism of their pathogenicity has not been clarified *in vivo* [17].

In the present study, osteoarthritis were created successfully in the radiocarpal joint through repeated injection of allogenous cartilage particle. Use of the 14 g needle facilitated the injection of the ACP. The eight ACP injection supported by exercise program to maintain the disease process over 70 day. Our model created a variety cartilage lesion grades ranged from surface irregularity to deep cartilage erosion that extended to the subchondral bone.

However horses have been described as a model to study osteoarthritis, this animal have some difficulties to work with as difficult on handling and operator safety, cost expensive in housing and feeding. Thus we should use an animal phylogenetically, biomechanically and biochemically close as is possible in order to most accurately reflect pathologic process in the target species [7]. Donkeys have many advantages as improved investigator safety, less size area for housing, allowing less stress, less requirements for exercise, identical anatomy with the horse, domesticated for low stress, lack of clinical research on the donkey, large joint size enable us to take a good amount of tissue for many histopathologic analysis.

Using of allogenous cartilage particles (ACP) to study OA had been described in previous studies. The mechanisms by which these particles help sustain inflammation and further erosion is controversial, but probably occurs by two mechanisms. First, cartilage particles may initially act as abrasives to liberate more 'wear particles' which are engulfed by the synovial membrane [26, 27] causing metaplastic changes in the membrane, abnormal synovial fluid constituents and synovitis. Secondly, cartilage particles may also stimulate synovial cells via immune system to produce cellular mediators and/or proteinases which result in depletion of cartilage matrix, either directly or by acting on the chondrocytes [28].

Dose selection was made upon our previous work on donkey where we use 50 mg/joint [12]. Our goal was to select the appropriate dose for creating a unique OA

model rather than the transient cartilage changes. Repeated injection and exercise were needed to accelerate a natural degenerative process that normally takes years to develop.

In the present study, intra-articular injection of allogenous cartilage particles effectively resulted in clinical, gross, histologic and biochemical changes indicative of osteoarthritis. The lesions are thought to represent both chronic synovitis and traditional osteoarthritis that includes full-thickness cartilage erosion. During this study, no adverse events were recorded with any of the treatment doses and a mild degree of lameness was induced (typically grade 2 on a scale published by the American College of Equine Practitioners) [18].

Lameness is often a feature of natural or experimentally induced OA. In some cases, lameness may be severe that limits usefulness of a model [29]. Despite the fact that articular cartilage degeneration was induced in our study, lameness was not a major feature of both groups. This mimics the natural occurring disease where the majority of the clinical cases were less severe.

In our study partial and full thickness cartilage erosion were observed in addition to synovial membrane adhesion and pannus formation, however in other study in the horse the lesions were limited to wear lines and areas of cartilage thinning together with capsular fibrosis and synovial membrane hyperplasia [13]. This may be due to low cartilage dose (10mg) and prolongation of the study period (6 months). While in other species synovitis, stiffness and marginal exostoses without damage to the articular surfaces could be detected grossly or microscopically [10] in contrast to Evans's study was concomitant destruction of articular cartilage [11].

This study agrees with other studies conducted on the cartilage particle injection reported synovial fibrosis [10] with small cartilage particles engulfed inside the synovial subintimal layer [11, 13]. However, other studies also reported synovial intimal hyperplasia [13].

In the present study, we demonstrate osteoarthritic cartilage surface for abnormal situations and assessment of cartilage surface in different osteoarthritis stages, which could facilitate comparisons among repair strategies. Our grading system are similar to Clark observations who summarized the Cartilage SEM lesions into four categories: Superficial Roughness, Subsurface Fissures, Superficial Fronding and Full-Thickness Fissures [23]. The SEM results validate the light microscopy results and offer a good method for assessing osteoarthritic cartilage.

Pathological study using OA models focused on changes in cartilage and bone. Our study was the first to examine the synovial membrane in osteoarthritic animal model. The novel observation was crystal deposition on the surface of synovial membrane, which has not reported previously in such condition in an OA model.

The origin of BCP crystals is not fully understood; however, both CPPD and HA crystals may be generated in matrix vesicles (MV) derived from articular cartilage [30]. There is histologic evidence of MV near BCP crystal deposits in the articular cartilage. Substances within the extracellular matrix (ECM) strongly influence the mineralizing activity of MV *in vivo* [31]. Another likely source of BCP crystals in advanced OA is the bony shards embedded in damaged cartilage and bony debris resulting from the exposure of subchondralbone due to cartilage erosion [32].

In our study, the large rosette shape crystals (0.5 mm) that adhere to the synovial membrane may be related to calcium phosphate crystals group however, it is not possible to identify the crystals by their shape as they need further spectroscopy or x-ray diffraction analysis.

These crystals may be formed by local cartilage matrix degeneration that enable the chondrocyte matrix vesicle to precipitate CPPD and apatite minerals. These mineral aggregations with cartilage debris are the nidus for the formed crystals. Many enzymes as; pyrophosphatase enzyme; adenosine triphosphate (ATP) and nucleotide pyrophosphohydrolase (NTPPH) may affect the type of the crystals. These enzymes are derived from degenerated chondrocytes, synoviocytes or plasma. Calcium phosphate crystals may form within MV where calcium and phosphorus may be concentrated in a site protected from other inhibitor of mineralization [33].

In our study rising of synovial fluid calcium, phosphorus and magnesium to certain concentration is indicator for crystal formation and joint destruction this idea may be a future diagnostic tool for diagnosis and monitoring osteoarthritis.

CONCLUSION

Repeated intra-articular injection of 100 mg/joint ACP cause cartilage erosion extend to break up the tidemark and accompanied by changes on the subchondral bone and crystals formation. This model may be useful for studying the disease process and the effect of the chondroprotective agent and crystal inhibitors on the cartilage healing as well as studying the origin and the pathway of joint crystals in joint disease.

Manufacturers' Addresses:

- I Eqvalan: (Oral Paste) 6.08g contains ivermectin 1.87% Merial Limited. USA.
- II Amikin.Bristol Meyer Squiip Egypt.
- III Rumpon: 50ml vial contains 5gm Xylazine HCL Bayer animal health. Canada.
- IV Nembutal Sodium: 20-mL vial contains 1000mg pentobarbital sodium. Lundbeck Inc. Deerfield, IL 60015. U.S.A.
- V JEOL JSM 5200LV electron microscope. Japan.
- VI IBM SPSS Statistics Version 23: IBM release 2015

ACKNOWLEDGEMENTS

Our very grateful thanks are extended to Dr. Margaret Smith for editing of the manuscript. We also thank Mr. Magdi Moustafa and Mr. Yassen Qura for preparation of the Light and Electron microscopy specimens.

Authors' Declaration of Interests: There are no conflicts of interest.

Sources of Funding: This work was done through a joint research project between Kafrelsheikh university, Egypt and Biopharm Pharmaceutical, Australia. The work performed was not influenced at any stage by the support provided.

REFERENCES

1. Brown, T.D., R.C. Johnston, C.L. Saltzman, J.L. Marsh and J.A. Buckwalter, 2006. Posttraumatic osteoarthritis: a first estimate of incidence, prevalence and burden of disease. *J. Orthop Trauma.* 20(10): 739-44.
2. Anderson, D.D., S. Chubinskaya, F. Guilak, J.A. Martin, T.R. Oegema, S.A. Olson and J.A. Buckwalter, 2011. Post-traumatic osteoarthritis: improved understanding and opportunities for early intervention. *J. Orthop Res.*, 29(6): 802-9.
3. Goldring, M.B. and S.R. Goldring, 2007. *Osteoarthritis.* *J. Cell Physiol.*, 213(3): 626-34.
4. Lawrence, R.C., D.T. Felson, C.G. Helmick, L.M. Arnold, H. Choi, R.A. Deyo, S. Gabriel, R. Hirsch, M.C. Hochberg, G.G. Hunder, J.M. Jordan, J.N. Katz, H.M. Kremers and F. Wolfe, 2008. Estimates of the prevalence of arthritis and other rheumatic conditions in the United States. Part II. *Arthritis Rheum.*, 58(1): 26-35.

5. Altman, R.D., S. Abramson, O. Bruyere, D. Clegg, G. Herrero-Beaumont, E. Maheu, R. Moskowitz, K. Pavelka and J.Y. Reginster, 2006. Commentary: osteoarthritis of the knee and glucosamine. *Osteoarthritis Cartilage*, 14(10): 963-6.
6. Little, C.B. and S. Zaki, 2012. What constitutes an “animal model of osteoarthritis” the need for consensus? *Osteoarthritis and Cartilage*, 20(4): 261-267.
7. May, S.A., 1996. Animal models and other experimental system in the investigation of equine arthritis, in *Joint Disease in the Horse*, C.W. McIlwraith and G.W. Trotter, Editors, W.B. Saunders, pp: 421-440.
8. Pritzker, K.P., 1994. Animal models for osteoarthritis: processes, problems and prospects. *Annals of the Rheumatic Diseases*, 53(6): 406.
9. McIlwraith, C.W., D.D. Frisbie and C.E. Kawcak, 2012. The horse as a model of naturally occurring osteoarthritis. *Bone Joint Res.*, 1(11): 297-309.
10. Chrisman, O.D., J.M. Fessel and W.O. Southwick, 1965. Experimental production of synovitis and marginal articular exostoses in the knee joints of dogs. *The Yale Journal of Biology and Medicine*, 37(5): 409.
11. Evans, C.H., R.A. Mazzocchi, D.D. Nelson and H.E. Rubash, 1984. Experimental arthritis induced by intraarticular injection of allogenic cartilaginous particles into rabbit knees. *Arthritis & Rheumatism*, 27(2): 200-207.
12. Elmesiry, A., M. Seleim and D. Cullis-Hill, 2014. Iodoacetate and allogenous cartilage particles as models for arthritis induction in equine. *International Journal of Veterinary Science and Medicine*, 2(2): 142-150.
13. Hurtig, M.B., 1988. Use of autogenous cartilage particles to create a model of naturally occurring degenerative joint disease in the horse. *Equine Veterinary Journal*, 20(s6): 19-22.
14. Huber, M.J., W.B. Schmotzer, T.W. Riebold, B.J. Watrous, S.P. Synder, E.A. Scott and P.C. von Matthiessen, 1992. Fate and effect of autogenous osteochondral fragments implanted in the middle carpal joint of horses. *American Journal of Veterinary Research*, 53(9): 1579-1588.
15. McCarthy, G.M. and H.S. Cheung, 2009. Point: Hydroxyapatite crystal deposition is intimately involved in the pathogenesis and progression of human osteoarthritis. *Curr. Rheumatol. Rep.*, 11(2): 141-7.
16. MacMullan, P., G. McMahon and G. McCarthy, 2011. Detection of basic calcium phosphate crystals in osteoarthritis. *Joint Bone Spine.*, 78(4): 358-63.
17. Jin, C., P. Frayssinet, R. Pelker, D. Cwirka, B. Hu, A. Vignery, S.C. Eisenbarth and R.A. Flavell, 2011. NLRP3 inflammasome plays a critical role in the pathogenesis of hydroxyapatite-associated arthropathy. *Proc. Natl. Acad. Sci. USA*, 108(36): 14867-72.
18. Baxster, G.M. and T.S. Stashak, 2011. Examination for Lameness, in *Adams and Stashak's Lameness in Horses*, G.M. Baxter, Editor, Wiley.
19. Toutain, P.L. and C.C. Cester, 2004. Pharmacokinetic-pharmacodynamic relationships and dose response to meloxicam in horses with induced arthritis in the right carpal joint. *American Journal of Veterinary Research*, 65(11): 1533-1541.
20. Steel, C.M., 2008. Equine synovial fluid analysis. *Veterinary Clinics of North America: Equine Practice*, 24(2): 437-454.
21. McIlwraith, C.W., D.D. Frisbie, C.E. Kawcak, C.J. Fuller, M. Hurtig and A. Cruz, 2010. The OARSI histopathology initiative- recommendations for histological assessments of osteoarthritis in the horse. *Osteoarthritis and Cartilage*, 18: S93-S105.
22. Pritzker, K.P.H., S. Gay, S.A. Jimenez, K. Ostergaard, J.P. Pelletier, P.A. Revell, D.V.D. Salter and W.B. Van Den Berg, 2006. Osteoarthritis cartilage histopathology: grading and staging. *Osteoarthritis and Cartilage*, 14(1): 13-29.
23. Clark, J.M. and P.T. Simonian, 1997. Scanning electron microscopy of “fibrillated” and “malacic” human articular cartilage: technical considerations. *Microscopy Research and Technique*, 37(4): 299-313.
24. Cheung, H.S., 2005. Role of calcium-containing crystals in osteoarthritis. *Front Biosci.*, 10: 1336-40.
25. Pritzker, K.P., 2009. Counterpoint: Hydroxyapatite crystal deposition is not intimately involved in the pathogenesis and progression of human osteoarthritis. *Curr. Rheumatol. Rep.*, 11(2): 148-53.
26. Evans, C.H., E.R. Bowen, J. Bowen, W.P. Tew and V.C. Westcott, 1980. Synovial fluid analysis by ferrography. *Journal of Biochemical and Biophysical Methods*, 2(1): 11-18.
27. Meachim, G., 1979. Ageing and degeneration, in *Adult articular cartilage*, M.A.R. Freeman, Editor, Pitman Medical, pp: 215-290.

28. Evans, C.H., D.C. Mears and J.L. Cosgrove, 1981. Release of neutral proteinases from mononuclear phagocytes and synovial cells in response to cartilaginous wear particles *in vitro*. *Biochimica et Biophysica Acta (BBA)-General Subjects*, 677(2): 287-294.
29. McIlwraith, C.W. and D.C. Van Sickle, 1981. Experimentally induced arthritis of the equine carpus: histologic and histochemical changes in the articular cartilage. *American Journal of Veterinary Research*, 42(2): 209-217.
30. Derfus, B., S. Kranendonk, N. Camacho, N. Mandel, V. Kushnaryov, K. Lynch and L. Ryan, 1998. Human osteoarthritic cartilage matrix vesicles generate both calcium pyrophosphate dihydrate and apatite *in vitro*. *Calcif Tissue Int.*, 63(3): 258-62.
31. Jubeck, B., C. Gohr, M. Fahey, E. Muth, M. Matthews, E. Mattson, C. Hirschmugl and A.K. Rosenthal, 2008. Promotion of articular cartilage matrix vesicle mineralization by type I collagen. *Arthritis Rheum.*, 58(9): 2809-17.
32. MacMullan, P., G. McMahon and G.M. McCarthy, 2012. Chapter 22 - Basic Calcium Phosphate Crystal Arthropathy, in *Gout & Other Crystal Arthropathies*, R. Terkeltaub, Editor, W.B. Saunders: Philadelphia, pp: 266-281.
33. Ea, H.K. and F. Liote, 2009. Advances in understanding calcium-containing crystal disease. *Curr. Opin. Rheumatol.*, 21(2): 150-7.